Microfluid Nanofluid (2008) 5:255–262
DOI 10.1007/s10404-007-0243-7

RESEARCH PAPER

Dual thermopile integrated microfluidic calorimeter for biochemical thermodynamics

B. S. Kwak · B. S. Kim · H. H. Cho · J. S. Park · H. I. Jung

Received: 11 September 2007 / Accepted: 12 November 2007 / Published online: 11 December 2007

Abstract This article presents a new design of a silicon-based microcalorimeter made with dual thermopiles and a microchannel. The dual thermopile was fabricated with chromium and copper using a microelectromechanical system (MEMS) technique, and the microchannel was made of PDMS using soft-lithography. Each thermopile consists of 26 thermocouple pairs and 50 μm wide electrodes. The total sensitivity of thermopile is 428 μV/K. The dual thermopile system enables the microcalorimeter to acquire reliable data in a rapid and convenient manner because it detects the reaction and reference temperatures simultaneously. This self-compensation allows our device to analyze a few microliters of sample solution without the need for a surrounding adiabatic vacuum.

Keywords Microchannel · Calorimeter · Dual thermopile · Biochemical reaction

1 Introduction

Microcalorimetry is a very useful technique in thermodynamic studies of complex biological processes, like protein–protein interactions, enzyme kinetics, and cell metabolism (Lerchner et al. 2006; Maskow et al. 2006; Cooper 2005). Silicon chip based microcalorimeters have been recently developed by microfabrication techniques. Miniaturized thermal sensors have many significant advantages in biochemical and clinical diagnostic applications: low cost, ease of use, fast response times, and no requirement of any labeling or immobilization of reagents. These devices are capable of analyzing small (microliter) quantities of sample (Lerchner et al. 2006) and the thermodynamics of whole cell biotransformations (Maskow et al. 2006; Lerchner et al. 2007). Many research groups have tried to improve the sensitivity and efficiency of the calorimeter by developing thermocouple materials and device configurations (Lerchner et al. 2006; Verhaegen et al. 2000). For instance, Verhaegen et al. (2000) have reported a highly sensitive (130 mV/K) microphysiometer and use it to measure the thermal changes in kidney cells of *Xenopus Laevis*. Other groups have demonstrated that a very small quantity of sample (<20 μl) can be used to measure enzyme catalyzed reactions using a PMMA microchannel (Baier et al. 2005), Pyrex7740 microfluidic reaction chamber (Zhang and Tadigadapa 2004), and split-flow technique for a calibration system (Yoon et al. 2006).

However, despite a great effort toward miniaturization and sensitivity increases of the thermal sensor, the practical application for medical diagnosis is limited since the calorimeter by itself requires an adiabatic system and small sample volume. In order to overcome such limitations, we now introduce a dual thermopile microcalorimeter. We use 26 pairs of Cr and Cu thermocouple in each thermopile, implemented in a microfluidic chip. Consequently, our device is self-compensated so that the typical surrounding adiabatic vacuum is no longer needed. In addition, our microfluidic system requires only a small amount of expensive biomaterials (which can be recycled). This novel design of a dual thermopile integrated into a microfludic chip has a great potential to be applied in medical diagnosis such as cancer detection.

B. S. Kwak · B. S. Kim · H. H. Cho · J. S. Park · H. I. Jung (✉)
School of Mechanical Engineering, Yonsei University,
Seoul, South Korea
e-mail: uridle7@yonsei.ac.kr

2 Materials and methods

2.1 Fabrication of a microthermopile

The Seebeck coefficients of chromium and copper are 21.8 and 1.83 μV/K at 300 K, respectively (Moore et al. 1977). We performed calibration process using nichrome heater wire and condenser. Temperatures of condenser, hot and cold junctions were monitored using three conventional J-type thermocouples. The condenser was set at 16°C, and the nichrome heater wire was located near the hot junction. The sensitivity of our device is obtained to be 428 μV/K. Our microthermopile has a reasonable sensitivity compared with standard metal thermocouples (30–50 μV/K) (Merzlyakov 2003). A microthermopile is fabricated on a silicon wafer using conventional wet chemical etching and photolithography. To prepare the device, four photomasks are required: two to make Cr and Cu electrodes, and the others to make a SU-8 and PDMS microchannel. The fabrication process consists of many steps as shown in Fig. 1. First (Fig. 1a), a p-type silicon wafer of 4 in. diameter is thermally oxidized to grow a 1 μm thick silicone-dioxide (SiO_2) layer. This oxide layer works as electrical and thermal insulation between the silicon wafer and the thermopile electrodes. Second (Fig. 1b), a 3,000 Å thick Cr layer is coated on the whole SiO_2 area using a physical vapor deposition process. A thin layer of positive photoresist (AZ4620) is coated on the Cr surface using a spin coater at 3,000 rpm. Using a contact mask aligner, a mask no. 1 is positioned on the surface of the photoresist, which is exposed to ultraviolet light. The exposed photoresist is removed by a developing solution (AZ300); this provides the definition of the mask feature. Then, the wafer is submerged in a Cr etchant to leave the Cr layer in the desired pattern. Third (Fig. 1c), a titanium (Ti) layer of 100 Å and a Cu layer of 1 μm are consecutively deposited on the surface of the silicon wafer patterned with Cr electrodes, using sputtering equipment. Note that the ultra-thin titanium layer is necessary to improve the adhesion between the Cu and Cr layers. The Seebeck effect in the Ti junction is probably negligible since the Ti layer is much thinner than the other elements and its electrical resistivity is relatively high (titanium 0.420 μΩ m and copper 16.78 nΩ m). The etching in Fig. 1b is repeated, this time using a mask no. 2, to make the Cu electrodes of the thermopile. The widths of all chromium and copper electrodes, as well as the gaps between them, are 50 μm. After finishing the fabrication of the thermopile, we cut the silicon wafer with a dicing saw for decent packaging.

2.2 Integration of dual thermopiles and a microchannel

Our microfluidic calorimeter is composed of dual thermopiles and a splitting microchannel to measure heats of biochemical reactions. The major purpose of a dual thermopile is to achieve self-compensation of measurement noise under non-adiabatic or absorbed conditions. One of the dual thermopiles is used to measure the heat generated by the biochemical reaction, and the other is used to monitor the thermal equilibrium state of the calorimeter as a reference. The structure of the proposed calorimeter is shown in Fig. 2. Both thermopiles are positioned in the middle of a wafer, and the series of junctions are parallel to each other, having intervals of 100 μm. The area of the dual thermopile sensor is 5.25-mm × 6.1-mm. A microchannel is built upon the dual thermopile sensor and is fabricated with a negative photoresist (SU-8 2100) and polydimethylsiloxane (PDMS) using soft-lithography. First (Fig. 1d), a SU-8 photoresist layer is coated on the surface of the thermopile wafer using a spin coater at 3,000 rpm. The thickness of SU-8 photoresist layer is 80 μm. Using a UV photomask no. 3 (which has a pattern of a microchannel), the undesired sections of SU-8 layer are neatly dissolved by a SU-8 developer (MicroChem). Second (Fig. 1e), a PDMS mold which is another part of microchannel is fabricated by soft-lithography (Fig. 1f, g). A photomask no. 4 is used in this time, and the concave

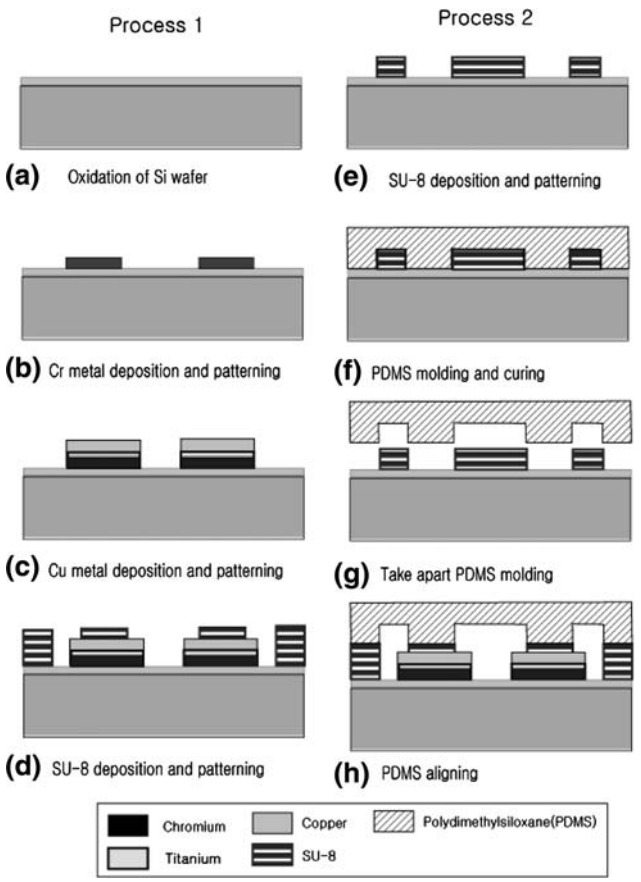

Fig. 1 Illustration of the fabrication procedure. Process 1 for the thermopile sensor and process 2 for the microchannel

surface of the PDMS mold has a depth of 100 μm. The PDMS mold is then attached on the SU-8 layer above the thermopile wafer (Fig. 1h). There are three reasons why the microchannel has a particular structure having a SU-8 layer. One, the alignment of the thermopile wafer and PDMS mold is easy and accurate. Second, the structure reduces leakage which may happen if the PDMS mold is directly attached on the thermopile surface. Third, the combination of SU-8 layer and PDMS mold gives rise to a relatively deep channel that allows an increase in the sample flow rate. After the PDMS mold is aligned on the dual thermopile wafer, a pressing frame is fabricated with two acryl glasses and screws in order to eliminate fluid leakage and heat transfer from the microchannel (Fig. 3).

The configuration of the microchannel was designed considering the need for an instantaneous infusion of three samples, an efficient mixing of samples, and appropriate dimensions of the dual thermopile sensors. Figure 2 shows the illustration of the microchannel integrated with the dual thermopile, which is applied in the microfluidic calorimeter. The microchannel consists of three inlets and outlets. Inlets I and III are split into two routes which are connected with inlet II. The split-joined inlets create three reaction channels where sample and buffer solutions are mixed. Reaction channels I and III are placed on two outside junctions of dual thermopiles separately, and as reaction channel II lies in the middle of dual thermopiles to cover two inside junctions. Unlike the fixed depth (180-μm) of the microchannel, widths vary according to position in the microchannel, i.e., three inlets 200 μm wide, reaction channels I and III 300 μm wide, and reaction channel II 400 μm wide. The dimensions of the whole structure are 36 mm × 28 mm.

2.3 Numerical and experimental analysis of flow injection

Prior to the experiments on thermal reactions, we conducted a flow injection analysis in order to identify the boundary conditions of inlet flows for the appropriate splitting and joining of the center and side streams as well as to verify the mixing characteristics of fluids in the microchannel using a commercial software of finite volume method (FVM), called Fluent 6.2.16. In these experiments, the flow in the microchannel is observed by using a microscope and a mixture of 1 M phenolphthalein and 1 M NaOH. This method uses the familiar color change of phenolphthalein upon addition of base. After phenolphthalein and NaOH flow into the center and side inlets separately, they are mixed at different locations in the microchannel according to the ratio of flow rates. By adjusting the flow rates, the two fluids will be mixed at the desired position which should exactly correspond to the reaction channel.

For a numerical analysis, we design the model based on two different kinds of liquids: water (H_2O) and methyl alcohol (CH_3OH) (which substitute for enzyme and substrate solutions) and calculate the behavior of the streams in the microchannel, allowing for mass diffusion between the two streams. The Reynolds number of the streams is very small, so the mass diffusion is the dominant mechanism in the fluid mixing process (Ottino 1989; Jen et al. 2003; Hong et al. 2004). Therefore, the simulation is modeled by solving the incompressible continuity equation, momentum conservation equations (Navier–Stokes equation) and mass diffusion equations. These equations can be expressed as the follows: (Kays et al. 2005)

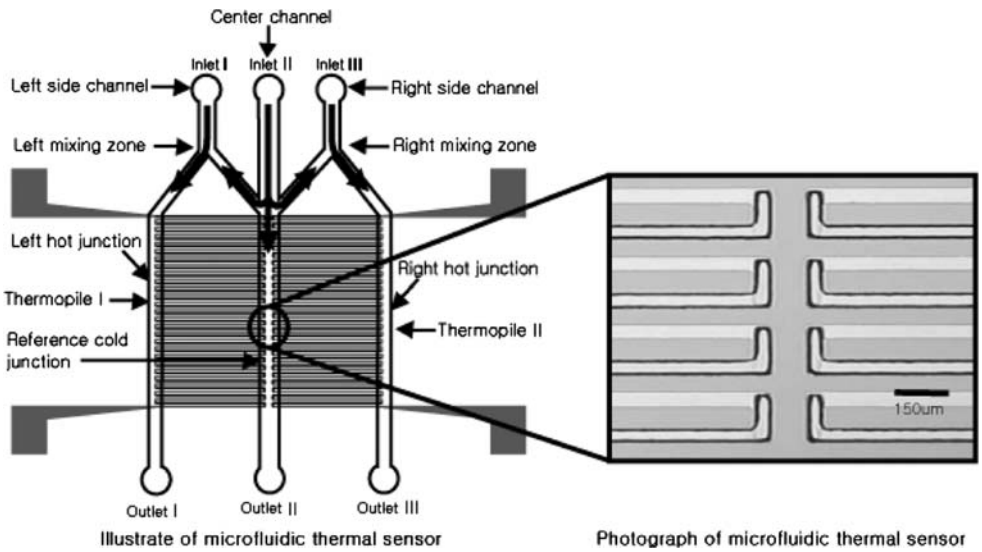

Fig. 2 Schematic illustration of our microfluidic calorimeter

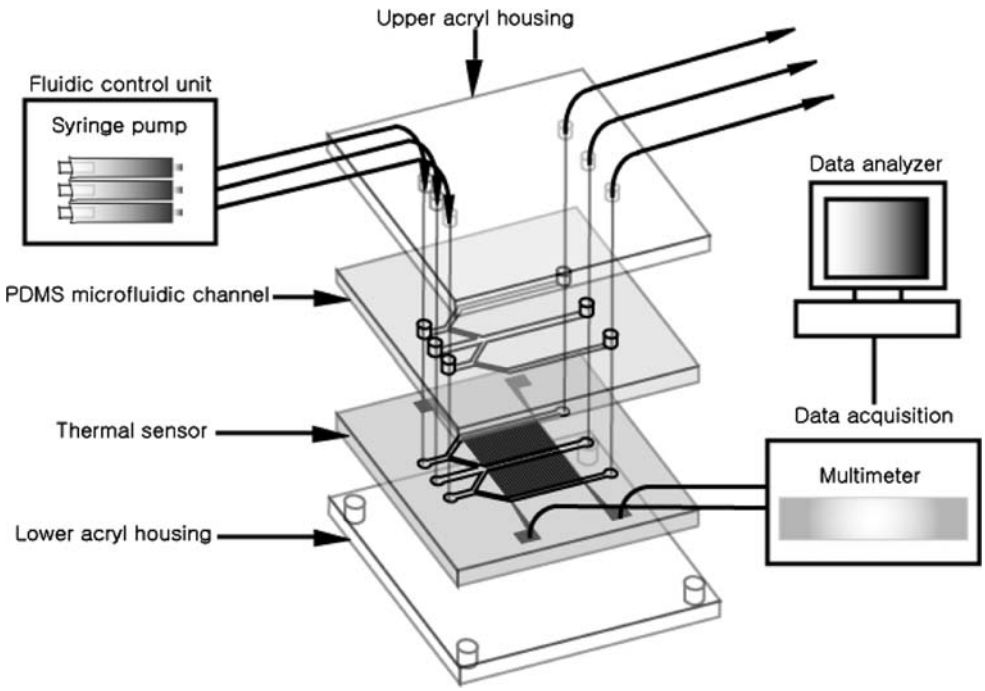

Fig. 3 Complete drawing of our device system

$$\nabla \cdot \overline{V} = 0 \tag{1}$$

$$\rho \frac{D\overline{V}}{Dt} = -\nabla p + \mu \nabla^2 \overline{V} \tag{2}$$

$$\overline{G} \cdot \nabla m_j - \nabla \cdot \gamma_j \nabla m_j = 0 \tag{3}$$

where $\gamma_j = \rho \overline{D}_j$, $\overline{D}_j = D_{12} = \cdots = D_{ij}.\overline{G}$, m_j and $\overline{D}_j$ represent mass flux vector (mass flow rate per unit of normal area), mass concentration of component j and mass diffusion coefficient, respectively.

Indeed, by changing the inlet velocities of center and side channels, we can obtain the appropriate experimental inlet boundary condition for the splitting and joining of the streams at the center and side channels, respectively. Water is injected through the inlet II and methyl alcohol is injected through the inlets I and III with the same inlet condition. We use physical properties of water and methyl alcohol at ambient temperature. To simulate the mass diffusion process between water and methyl alcohol, we apply mass diffusion coefficient (D_{ij}) of 1.09375×10^{-9} m^2 s^{-1} using the Schmidt number and property tables as referenced (Mills 1999). The Schmidt number, Sc is defined as the following:

$$\mathrm{Sc} = \frac{v}{D_{ij}} = \frac{\mu}{\rho D_{ij}}. \tag{4}$$

2.4 Measurement of a biochemical reaction

The microcalorimeter is equipped with TYGON tube of inner diameter 1/32 in. (Saint-Gobain Performance Plastics Co.) which is used to supply the sample fluids into the microchannel. The PDMS mold of the microcalorimeter has holes made by a punch at the ends of the microchannels to connect to the tubes. The tubes of three inlet channels are individually affixed on three syringes of syringe infusion pumps (KDS scientific, KDS210) which should provide micro flow rates with high precision (Fig. 3). It is very important to establish three steady flows by the pumps for carrying out the accurate flow-injection analysis. The three outlets of microchannel are also equipped with three tubes, through which the sample fluids are removed. Electrical wiring soldered to the dual thermopiles of the calorimeter leads to a micro voltmeter, which is connected to a PC for data acquisition, evaluation, and storage.

To demonstrate the performance of the microfluidic calorimeter, an enzyme-substrate reaction was performed. The substrate is L-ascorbic acid (Sigma–Aldrich) (A5960), and the enzyme is ascorbate oxidase (Sigma–Aldrich) (A0157), extracted from *Cucurbita* sp. Ascorbate oxidase catalyzes the oxidation of L-ascorbic acid:

$$\begin{aligned} &2\text{L-ascorbic acid} + \mathrm{O_2} \xrightarrow{\text{ascorbate oxidase}} \\ &\qquad 2\text{L-dehydroascorbic acid} + 2\mathrm{H_2O} \end{aligned} \tag{5}$$

The ascorbate oxidase (125 U/ml) is prepared with phosphate buffered saline solution (PBS, pH 5.6). Four concentrations (0.5, 1, 2, and 4 mmol/l) of L-ascorbic acid are prepared with the same PBS for measuring the output voltage change. The reason to use the same PBS in both enzyme and substrate solutions is to avoid the inequality of thermal properties of different buffer solutions.

3 Results and discussion

3.1 Micro flow injection analysis

3.1.1 Numerical method

We performed numerical analysis using different inlet flow rates at the inlet points to predict the flow and mixing locations of the streams. Basically, we found that if the mass flow rate of inlet II is higher than those of inlets I and III, the flow injected to a center channel is divided to three streams at the point A and is combined with the other flow at the point B (Fig. 4a). This numerical analysis agrees very well with the experimental observations. After simulations were repeated with variable flow rates of three inlets, we could obtain the suitable of inlets flow rates. We designed the volumetric flow conditions of 1 and 6 μl/min at the side inlets and the center inlet, respectively. In this case, each side channel has a Reynolds number of 0.12, and the center channel has one of 0.51. In Fig. 4b, c, the simulation result clearly shows that the stream injected through the inlet II splits into three streams, and one of these streams flows to a side channel and starts to mix with another fluid. In Fig. 4c, d, the efficiency of the mass diffusion through the reaction channel is shown by comparing the mixing of two fluids at the point B (the start of the reaction channel) and the point C (the end of the reaction channel). According to the simulation, the microchannel can achieve nearly full mixing using experimentally reasonable flow conditions and the dimensions of our reaction channel.

3.1.2 Experimental method

We observed five designated positions of the microchannel to identify the mixing flow: a split channel in inlet I

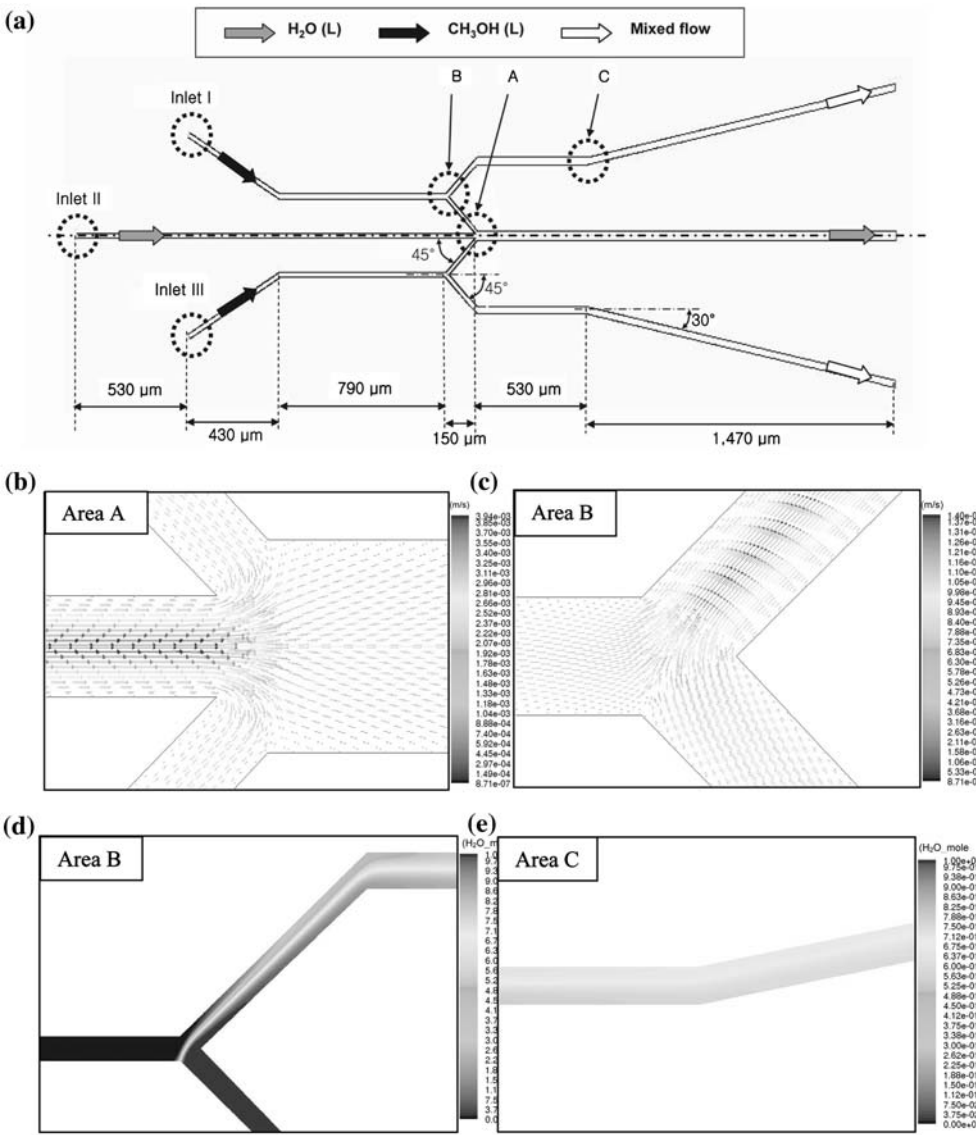

Fig. 4 Numerical analysis of the fluid dynamics in the microchannel. (**a**) Configuration of microchannel, (**b**) velocity vectors at point A, (**c**) velocity vectors at point B, (**d**) mole fraction of H_2O at point B, and (**e**) mole fraction of H_2O at point C

(Fig. 5I), a split channel in inlet III (Fig. 5II), a reaction channel on the hot junction of thermopile I (Fig. 5III), a split channel in inlet II (Fig. 5IV), and a reaction channel on the hot junction of thermopile II (Fig. 5V). Phenolphthalein was introduced into inlets I and III, and NaOH into inlet II. As shown in Fig. 5, the different colors in the designated positions represent that phenolphthalein flows from the center channel to the side channels and is mixed with NaOH at the split channels of inlets I and III. Since a center reaction channel is occupied by one fluid, it is used as a reference channel, or so-called cold junction. Based on optical observations, we found that a very stable mixing was produced at the split channels when a ratio between the center inlet's and the side inlets' flow rates is 6:1 (a ratio of less than 3:1 makes fluid from the two side inlets come into the center reaction channel). A ratio higher than 10:1 is not acceptable because at this relative flow rate, the back pressure from the center channel entry point prevents side channel fluid from entering the mixing zone. Consequently, the optimal ratio of 6:1 results in the almost 1:1 volume mixture of two fluids in the reaction channel.

3.2 Sensitivity of the dual thermopile microcalorimeter

We performed a preliminary experiment to verify the coincident response and sensitivity of the dual thermopiles of our calorimeter. L-Ascorbic acid of 2 mM was inserted into the inlets I and III with a flow-rate of 0 and 1 μl/min. At the same time, 125 U/ml ascorbate oxidase was inserted into the inlet II at a constant flow rate of 6 μl/min. Thermopiles I and II simultaneously measured output voltages due to the thermal difference between the hot junction heated by the reaction and the cold junction which has a temperature of the fluid injected through the inlet II. Figure 6 shows that dual thermopiles of our microfluidic calorimeter coincidently respond to the varying flow-rate of L-ascorbic acid. Based on the coincident response of dual thermopiles, one thermopile will be used as a reference sensor and the other as a measurement sensor.

3.3 Measurement of micro-heat from an enzymatic reaction

To test a biological application of our microfluidic calorimeter we measured output voltages of an enzymatic reaction at various concentrations of substrate. This demonstration uses L-ascorbic acid, ascorbate oxidase, and PBS buffer, which are inserted into inlets I, II, and III, respectively. In the reaction channel, the oxidation of L-ascorbic acid by ascorbate oxidase generated an electrical signal in the first thermopile. We used the solution of L-ascorbic acid as a reference; the second reaction channel generated a signal of approximately zero due to the lack of a chemical reaction. All experiments were performed at 22°C without external temperature control systems, and all temperatures were measured using conventional J-Type thermocouples. Figure 7 presents the raw data representing the electrical signals in both channels for 10 min. The voltage drop in the measurement thermopile occurred at the moment of L-ascorbic acid's injection. The applied volumes of L-ascorbic acid and enzyme were about 10 and 60 μl, respectively.

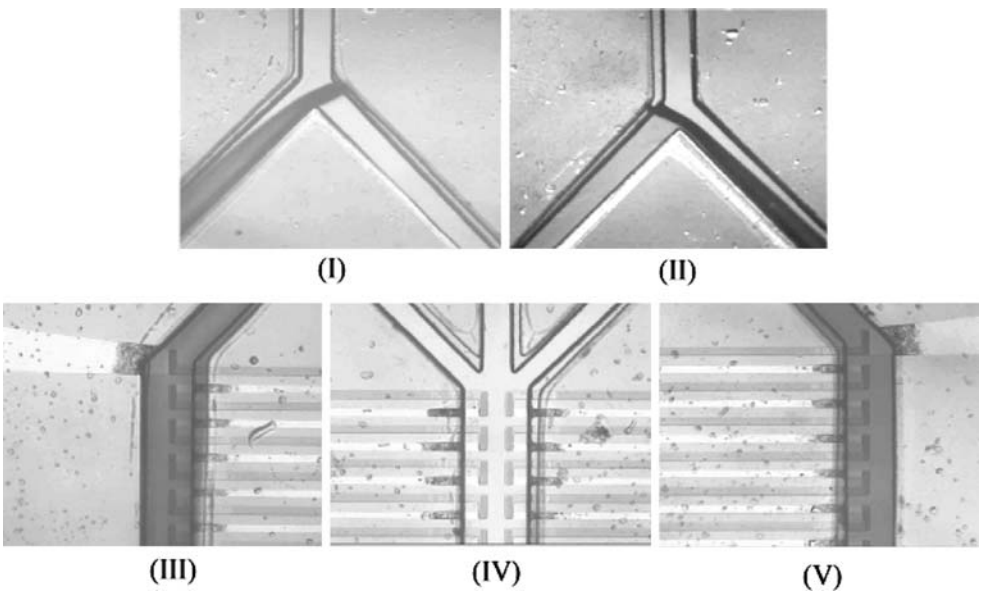

Fig. 5 Experimental analysis of mixing in the microchannel. We used 1 M phenolphthalein and NaOH solutions

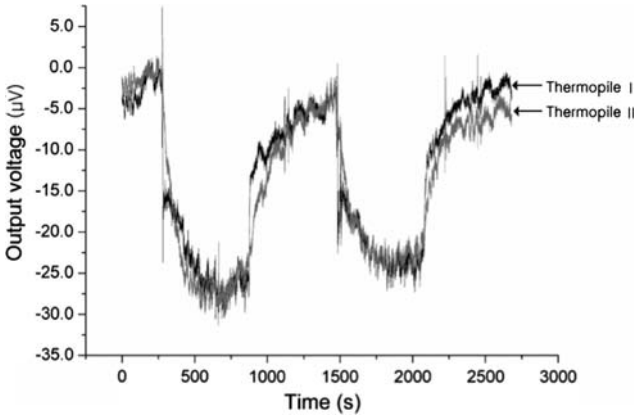

Fig. 6 Coincident output signals of dual thermopiles with flow rates of 1 μl/min at inlets I and III, and 6 μl/min at inlet II (Inlet I, III: 2 mM L-ascorbic acid, Inlet III: 125 U/ml ascorbate oxidase)

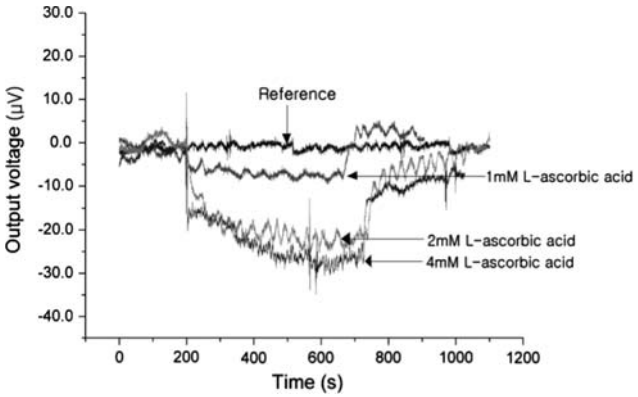

Fig. 7 Raw data of output signals that represent calories due to the oxidation of L-ascorbic acid by ascorbate oxidase under a various concentrations of L-ascorbic acid

Figure 8 shows that the output voltage increases proportionally to the sample concentration and is saturated at about 2 mM. Total volume of reaction area is 0.315 mm^3 and the staying period of samples in microchannel are 7–8 s. Most chemical reaction occurred within about 1 s because two different samples were fully mixed at the end of reaction channel. The reaction rate of enzyme was 125 U/ml that can dissolve the substrates of 125 μmol/ml (equivalent to 125 mM) per minute. Based on the actual interaction time of 1 s, the enzyme in the microfluidic system can catalyze L-ascorbic acids up to 2 mM. The maximum output voltage obtained from this experiment is around 25 μV. The sensitivity of our microfluidic calorimeter is 428 μV/K and the temperature change according to the maximum output voltage is 0.0584 K. The uncertainty of the calorimeter caused by unstable infusion rates from the micro syringe pump, inaccuracy of multimeter and irregularity in the dimensions of the microchannel is presumed to be around ±4 μV, which corresponds to ±0.0093 K with a confidence level of 99% and a coverage

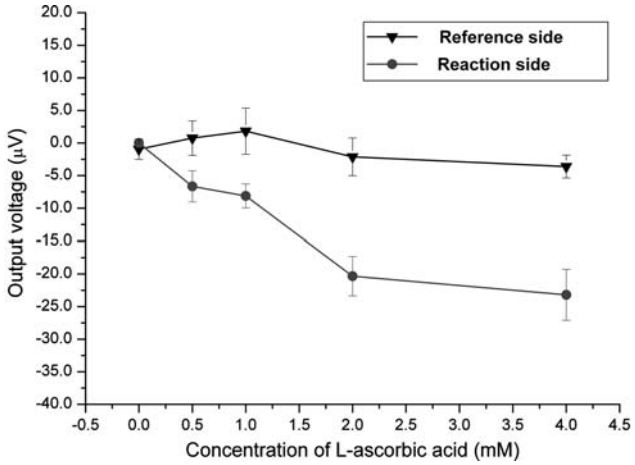

Fig. 8 Measurements obtained by dual thermopiles with various concentrations of L-ascorbic acid

factor of 2.58. It is very desirable to get a significant change of output voltage according to concentration by using a small number of thermopile junction pairs. In fact, the presence of a reference thermopile makes our calorimeter self-compensating and the average signal to noise ratio is 7.4. It is high enough to distinguish the signal from reference line noise. In the experiment, the thermopile did not start to acquire data until the reference thermopile remained at a moderate output of around zero voltage. Additionally, our calorimeter does not need any insulation system because we can measure the reaction and reference temperatures at the same time. In addition, the sample in the center channel does not react with any fluid, so it can be recycled. Biological samples can be very expensive; therefore, the reuse of samples is one of the promising advantages of our device.

4 Conclusions

In this article, we successfully demonstrated a novel design of a dual thermopile based microcalorimeter which can measure a biochemical reaction and a reference temperature simultaneously. Our thermal sensor can accomplish stable sensitivity of 428 μV/K with 26 thermocouple junction pairs in each thermopile. The use of dual thermopiles eliminates the requirement for a surrounding adiabatic vacuum and a heater for the calibration of inlet samples. In addition, the microfluidic system allows sample sizes on the order of 10 μl. The small volume limit of our device enables fundamental and extensive studies of even very expensive biochemical reactions.

Acknowledgments This work was supported by Basic Research Program of the Korea Science & Engineering Foundation (Grant no. R01-2005-000-10160-0(2006)), ICBIN of Seoul R&BD program

(Grant no. 10816), and National Core Research Center for Nanomedical Technology of the Korea Science & Engineering Foundation (Grant no. R15-2004-024-01001-0).

References

Baier V, Födisch R, Ihring A, Kessler E, Lerchner J, Wolf G, Köhler JM, Nietzsch M, Krügel M (2005) Highly sensitive thermopile heat power sensor for micro-fluid calorimetry of biochemical process. Sens Actuators A Phys 123:354–359

Cooper A (2005) Heat capacity effects in protein folding and ligand binding: a re-evaluation of the role of water in biomolecular thermodynamics. Biophys Chem 115:89–97

Hong CC, Choi JW, Ahn CH (2004) A novel in-plane passive microfluidic mixer with modified Tesla structures. Lab Chip 4:109–113

Jen CP, Wu CY, Lin YC, Wu CY (2003) Design and simulation of the micromixer with chaotic advection in twisted microchannels. Lab Chip 3:77–81

Kays WM, Crawford ME, Bernhard W (2005) Convective heat and mass transfer, 4th edn. McGraw Hill, New York

Lerchner J, Maskow T, Wolf G Chip calorimetry and its use for biochemical and cell biological investigations. Chem Eng Process (in press). doi:10.1016/j.cep.2007.02.014

Lerchner J, Wolf A, Wolf G, Baier V, Kessler E, Nietzsch M, Krügel M (2006) A new micro-fluid chip calorimeter for biochemical applications. J Thermochim Acta 445:144–150

Maskow T, Lerchner J, Peitzsch M, Harms H, Wolf G (2006) Chip calorimeter for the monitoring of whole cell biotransformation. J Biotechnol 122:431–442

Merzlyakov M (2003) Integrated circuit thermopile as a new type of temperature modulated calorimeter. J Thermochim Acta 403:65–81

Mills AF (1999) Basic heat and mass transfer, 2nd edn. Prentice Hall, New Jersey

Moore JP, Williams RK, Graves RS (1997) Thermal conductivity, electrical resistivity, and Seebeck coefficient of high-purity chromium from 280 to 1000 K. J Appl Phys 48(2):610–617

Ottino JM (1989) The kinematics of mixing: stretching, chaos, and transport. Cambridge University Press, Cambridge

Verhaegen K, Baert K, Simaels J, Driessche WV (2000) A high-throughput silicon microphysiometer. Sens Actuators A Phys 82:186–190

Yoon SI, Park SC, Kim YJ (2006) A microcalorimeter based on split-flow microchannel for biochemical applications with no-calibration. 20th EURO Sens 1:416–417

Zhang Y, Tadigadapa S (2004) Calorimetric biosensors with integrated microfluidic channels. Biosens Bioelectron 19:1733–1743